PROCEEDINGS, Seventeenth Workshop on Geothermal Reservoir Engineering
Stanford University, Stanford, California, January 29-31, 1992
SGP-TR-141

AN ACCURATE PVT MODEL FOR GEOTHERMAL FLUIDS AS REPRESENTED BY H_2O-CO_2-NaCl MIXTURES

G. Andersen, A. Probst, L. Murray, S. Butler

Unocal Science & Technology
376 S. Valencia
Brea, CA 92621

ABSTRACT

Estimates for the pressure decline in high TDS geothermal fluids containing dissolved gases are extremely sensitive to the PVT representation of the reservoir fluid. Significant errors in predicted pressures will occur if the geothermal fluid is represented by one or two pseudo components with modified water properties. As a result, we have developed a PVT model to predict the thermodynamic properties of a prototype geothermal fluid as represented by three-component H_2O-CO_2-NaCl mixtures. The range of applicability of the model is: Temperatures from 75 to 700+°F, pressures from 14.7 to 5000 psi, carbon dioxide content from 0 - 5 wt%, and salt concentrations to 30 wt%.

The model has been implemented into Unocal's version of a commercially available reservoir simulator and is currently being used to study one of Unocal's high salinity reservoirs located in the Imperial Valley of California.

INTRODUCTION

The first geothermal fields to be commercially exploited contained essentially hot water and steam. As a result, lumped and distributed parameter reservoir simulation models have provided reasonable performance predictions using steam table thermodynamic data.

More recently, a number of reservoirs have come under development in which the reservoir fluid can not be adequately represented by pure water with the most obvious examples being the Salton Sea and Broadlands fields in the United States and New Zealand respectively. These fields contains large quantities of either dissolved solids or non-condensable gases, components which substantially alter the thermodynamic behavior of the reservoir fluid. Preliminary modeling by our engineers and others have indicated that the presence of both components can drastically alter the pressure decline of a reservoir through their impact on the saturation pressure of the fluid. However, these previous studies have used models of the liquid-vapor equilibria that are severely limited in the range of pressures, temperatures and compositions that can be considered. Additionally, no systematic effort has been undertaken to test the accuracy of these models against the large quantity of known experimental data on these systems.

Unocal recognizes that accurate reservoir modeling of their geothermal resources has to explicitly take into account the multicomponent nature of the reservoir fluid. As a result we have developed a thermodynamic model which can represent the thermodynamic behavior of a prototype geothermal fluid as represented by mixtures of water, carbon dioxide and sodium chloride. The model has been tested against a wide class of literature data on H_2O-NaCl, H_2O-CO_2, and H_2O-CO_2-NaCl mixtures and accurately reproduces the known saturation pressures, densities and enthalpies at conditions appropriate to most known geothermal fields. This model has been implemented into a commercially available geothermal reservoir simulator and is currently being used to model the Salton Sea reservoir located in California's Imperial Valley.

PHASE EQUILIBRIUM CALCULATIONS

The presence of two coexisting phases in the reservoir has a dramatic effect on the reservoir pressure decline and the production well enthalpies. Thus, in reservoir modeling it is essential to accurately determine the quantity and composition of the liquid and vapor phases. This is performed through a combination of heat, material balance and phase equilibrium conditions.

The Condition for Phase Equilibria:

A requirement of phase equilibrium in any two-component liquid-vapor system is the equality of the chemical potential, or fugacity, of the components in the two phases:

$$f_i^l = f_i^g \qquad (1)$$

where i indicates a given component and l and g refers to the liquid and vapor phases respectively. The individual fugacities can be written as follows:

$$f^{v}_{co2} = P \cdot y_{CO2} \cdot \phi_{CO2} \quad (2a)$$

$$f^{l}_{co2} = H_{sat} \cdot x_{CO2} \cdot \gamma_{CO2} \cdot Pc_{CO2} \quad (2b)$$

$$f^{l}_{h2o} = P_{sat} \cdot \phi_{sat} \cdot a_{H2O} \cdot Pc_{H2O} \quad (2c)$$

$$f^{v}_{h2o} = P \cdot y_{H2O} \cdot \phi_{H2O} \quad (2d)$$

where

P = System pressure

y_{CO2} = CO_2 mole fraction in the vapor phase

ϕ_{CO2} = Vapor phase fugacity coefficient for CO_2

H_{sat} = Henry's law constant along the water saturation line

x_{CO2} = CO_2 mole fraction in the liquid phase

γ_{CO2} = Liquid phase activity coefficient for CO_2

Pc_{CO2} = Poynting correction for CO_2

P_{sat} = Saturation pressure of H_2O

ϕ_{sat} = Fugacity coefficient of H_2O at P_{sat}

ϕ_{H2O} = Vapor phase fugacity coefficient for H_2O

a_{H2O} = Liquid phase activity for H_2O

Pc_{H2O} = Poynting correction for H_2O

The APPENDIX lists the functional forms for most of the above listed variables.

The approach summarized in EQUATIONS 2a-d has been quite successful in correlating gas solubilities in a wide class of systems(Prausnitz, 1986). The model assumes a reference condition that is centered on the pure solvent with most of the terms in EQUATION 1 being correction factors calculated from this point. It is these correction factors that have been generally ignored in previous studies. Additionally, previous works have used correlations for the temperature dependence of the Henry's law constant that have questionable accuracy above 600°F. In the present model we describe a method for linearizing the temperature dependence of H_{sat} which allows the function to be accurately extended up to the critical point of water.

The above thermodynamic model does have limitations with respect to geothermal applications. Quantities such as the saturation pressure and Henry's law constant in EQUATION 2 are formally defined only for temperatures below the critical point of the solvent which, for H_2O, is approximately 700°F. For geothermal systems containing high levels of dissolved solids the reservoir temperature can exceed this value. Our experience has shown that our correlations for those previously mentioned properties appear to be extrapolatable and give reasonable results for many thermodynamic properties up to approximately 750°F.

We also recognize that the above approach is probably not appropriate for describing near critical mixtures. For these situations we feel that equations of states which assume a continuity between liquid and vapor phases will provide a better description. As of this time, this has not been a limitation in our reservoir modeling.

H_2O-NaCl SYSTEM

Bubble Point Pressures

For the two-component H_2O-NaCl system the change in the vapor pressure from its pure water value is accounted for in the composition dependence of the activity of water. The activity was fit to the saturation pressures reported by Haas(1976), Pitzer(1984), and Bischoff(1989). In FIGURE 1 we compare model predictions for the saturation pressure at a series of sodium chloride concentrations with that reported by Haas for temperatures up to 575°F. The maximum deviation is less than 1%. For more extreme conditions comparisons are with the data from Bischoff and Pitzer. At the highest temperature and salt concentration the error is around 2%. These results indicate that the model can accurately reproduce the experimental saturation pressures up to 750°F.

CO_2-H_2O SYSTEM

Experimental Data:

The data used to construct and test the model was obtained from six different sources and spans temperatures from 60 to 660°F and pressures from 20 to 50,000 psi. These data contain measurements of carbon dioxide solubility at conditions that cover

most known geothermal reservoir conditions of pressure, temperature and CO_2 concentration. All of the available data at pressures less than 5000 psi has been used to test the model.

Henry's Law Constant

The calculation of the solubility of CO_2 in water is primarily determined by the Henry's Law constant H_{sat}. The experimental data available on H_{sat} are not entirely consistent, particularly at higher temperatures. FIGURE 2 presents the reported Henry's law constants, and those calculated by ourselves for the data of Takenouchi(1964) and Toedheide(1963), as a function of temperature. The maximum in the Henry's Law constant at approximately 300°F is a feature common to slightly soluble gases. It presents difficulties in developing a simple empirical correlation that can be accurately extrapolated to higher temperatures. As a result we have used an approach recently developed by Harvey & Levelt-Sengers(1990) which expresses the Henry's constant as a function of the density of the solvent. The exact form of the correlation is given in the Appendix. In FIGURE 3 we compare calculated versus observed Henry's law constants for CO_2 along the saturation line of pure water.

Vapor-Phase Fugacity Coefficients, Poynting Corrections and Activity Coefficients

Fugacity coefficients were initially calculated using the Peng-Robinson(Peng, 1980) equation-of-state. In order to minimize the computational overhead in the reservoir simulator we also evaluated using a composition independent correlation for the fugacity coefficient. The correlation provided minimal degradation in accuracy from the equation-of-state solution and as a result, all phase equilibrium calculations were performed using the latter. Apparent molar volumes of CO_2 for the Poynting correction and activity coefficient parameters for CO_2 in pure water were obtained from the literature.

Saturation and Bubble Point Pressures

We also compared model predictions for the equilibrium saturation pressures with the reported values. Model results were generated from the reported liquid-phase compositions. This is shown in FIGURE 4 where the deviation between model predictions and the data is less than 5% for the majority of the measurements. At higher temperatures the data is less certain and the error can be as large as 15%.

Zawisza(1981) provided information on the bubble point pressure in the carbon dioxide-water system over the temperature range of 120-400°F and the pressure range of 20-800 psi. Experimental versus predicted results are shown in FIGURE 5 and the agreement has a standard deviation of 5%.

Dew Point Pressures

Zawisza also determined the dew point pressures for a number of different H_2O-CO_2 mixtures. In TABLE 1 we show that model predictions are in good agreement with the data at two compositions, at three different temperatures.

TABLE 1

T °F	y_{CO2}	P_{exp}(psi)	P_{model}(psi)	Error (%)
392	0.065	239.5	241.8	1.0
347	0.065	135.3	138.5	2.3
392	0.297	328.4	331.1	0.8
347	0.297	189.6	187.6	1.1
302	0.297	96.9	99.0	2.2

H_2O-CO_2-NaCl SYSTEM

Extending the model from the two-component systems to three components involves including the effect of NaCl on the activity coefficient of CO_2. The actual form of the activity coefficient is given in the Appendix and is derived from the data of Ellis et. al. as reported by Mason and Kao(1980).

Bubble Point Pressures

FIGURE 6 compares the predicted equilibrium pressure of two-phase solutions to the experimental data of Ellis @ Golding(1963) which spans concentrations from 0 to 10.5 wt % NaCl and 0 to 5 wt % CO2. The standard deviation between the model's predictions and the experimental data is approximately 5%. The predicted pressures are somewhat lower than those reported by Ellis. This was expected since Ellis's Henry's Law constant was consistently lower than those predicted by the model.

In FIGURE 7 we compare model predictions for the bubble point pressures in the three-component system with the data of Gehrig(1980) for a 6 wt % NaCl solution with 0.42 and 8.4 wt % CO_2. At the lower CO_2 concentrations there is good agreement between model and experimental data at all temperatures. At the higher CO_2 concentrations the agreement degrades. However, this pressure and concentration of CO_2 is well above what is normally seen in two-phase geothermal reservoirs but was included to show that, even in extreme cases, the model

gives good qualitative predictions of the experimental data.

Gehrig also measured a few data points at higher salt concentrations. Model predictions versus experimental results for those conditions are given in TABLE 2 where compositions are expressed in weight percent.

TABLE 2

T(°F)	x_{NaCl}	x_{CO2}	P_{model}(psi)	P_{exp}(psi)	Error(%)
619	9.5	4.7	4200	4400	-4.8
536	19.9	0.6	1800	1700	5.5
701	19.9	0.6	3300	3400	-3.0

These results indicate that the model provides reasonable predictions for the saturation pressure at NaCl concentrations significantly greater than those covered in the Ellis experiments. The latter were used to determine the NaCl dependence of the activity coefficient of CO_2 in the model.

VAPOR-PHASE DENSITY

The density of the two-component vapor-phase composed of CO_2 and H_2O is calculated using a four parameter cubic equation-of-state developed by P. K. Vinsome(1991). FIGURE 8 compares the predicted vapor densities for pure water vapor at the saturation pressure to steam table data (Burnham, 1969). Predicted densities for pure carbon dioxide at the saturation pressure of water are also compared to the experimental data of Chen(1959). Predicted densities for carbon dioxide are in good agreement with the experimental data over the entire range of temperatures considered. Predicted steam densities agree with the steam table data to approximately 675°F. However, as the temperature approaches the critical point the density estimate is less accurate.

LIQUID-PHASE DENSITY

A variety of approaches were evaluated for modeling the liquid density. The first method considered was that used by our reservoir simulator which expresses the volume of the solution as a sum of partial molar volumes of the individual components

$$V = \Sigma\, x_i \cdot \nu_i^\circ \cdot (1.0 + C_i \cdot (P - P_{sat})) \qquad (3)$$

where, V is the liquid volume and x_i, ν_i° and C_i are the mole fraction, saturated partial molar volume and compressibility factor for each component. The term $(P-P_{sat})$ is the deviation of the pressure from its saturation value. Notice that the pressure dependence is represented by linearized compressibility factors of the individual components.

H_2O-CO_2

The effect of CO_2 on the liquid phase density was calculated using EQUATION 3. Essentially no information is available on the effect of CO_2 on the compressibility of the liquid phase. We neglect this effect by assuming that the fluid compresses as if the CO_2 were not present.

NaCl-H_2O

While EQUATION 3 works well over a broad range of temperatures for the above two-component system, problems were encountered with the method for small salt concentrations near the critical temperature of water. In that region of the phase diagram the system is extremely compressible and the partial molar volume of NaCl approaches negative infinity. An alternative approach that gave good results for all concentrations and temperatures was a corresponding states-like expression in which the molar volume of the salt solution along the saturation line is expressed in terms of a function of the reduced temperature ($T/T_{critical}$) of the mixture. The expression used was similar to that of Torquato and Stell(1982) and accurately reproduces the experimental density of water up to its critical point. A correlation for the critical temperature of sodium chloride solutions was derived from the data of Marshall and Jones(1974). The experimental density data of Potter(1978) was then used to fit the one remaining adjustable parameter in the correlation. The compressibility factor for the NaCl solution was also correlated to the reduced temperature of the mixture using the Potter data at 4350 psi. The derivation of these correlations is detailed in the APPENDIX.

FIGURE 9 compares the model predicted densities to experimental data for the pure water and two-component system at various NaCl concentrations. The density correlation accurately reproduces the water data to the critical point, 705°F. and is within 1% of the experimental data of sodium chloride brines to 800°F. Errors are slightly higher for low salinity solutions at higher temperatures.

NaCl-H_2O-CO_2

The effect of CO_2 on a NaCl-H_2O liquid phase density was calculated using EQUATION 3 assuming that the partial molar volume of CO_2 was equal to its pure water value. This is a reasonable assumption except near the critical temperature of

water. Due to its low solubility, carbon dioxide has only a marginal impact on the brine density. At 200°F, the addition of 1.0 weight percent carbon dioxide increases the density of a 30 wt% NaCl solution by 0.3%.

LIQUID-PHASE ENTHALPY

$NaCl-H_2O$

For both the liquid and vapor phases we assume the enthalpy is given by

$$H = \Sigma\, x_i \cdot H_i \qquad (4)$$

where, x_i and H_i are the mole fraction and partial molar enthalpy of each component. As for the densities, we assume the enthalpy of the water-NaCl component is given by a corresponding states-like expression. The actual functional form is given in the appendix and the adjustable parameters were fit to the data of Haas(1976). The partial molar enthalpy of CO_2 in the liquid is obtained from the appropriate temperature derivative of its K value combined with the CO_2 vapor phase enthalpy.

FIGURE 10 shows the comparison of the experimental and predicted enthalpies for the $NaCl-H_2O$ system. Pure water enthalpies are accurately reproduced to the critical point of water. Model generated brine enthalpies are within 1% of the experimental data from 250 to 600°F. At lower temperatures, the discrepancy between the predicted and experimental values is somewhat larger. At higher temperatures model predictions agree with those of the recently developed Tanger(1989) equation-of-state for $NaCl-H_2O$ mixtures.

VAPOR-PHASE ENTHALPY

We assume that NaCl does not partition into the vapor phase and the remaining two partial molar enthalpies are approximated by their pure component vapor-phase values. The detailed correlations for each component are given in the APPENDIX. Experimental and predicted enthalpies for CO_2 in the vapor phase are compared in FIGURE 11. All enthalpy predictions are well within 1% of the experimental values. Experimental and predicted enthalpies for steam and water are compared in FIGURE 12. The agreement with the experimental data is excellent over the temperature range 25-700°F.

CONCLUSIONS

The model described above provides accurate predictions of the thermodynamic of mixtures containing H_2O, CO_2 and NaCl for temperatures in excess of 600°F and NaCl concentrations up to 20 wt %. Model predictions at higher temperatures and salt concentrations in the three-component system have not been verified due to the lack of experimental data. We are currently starting an experimental program that will obtain such data. The model is sufficiently general that it can be specifically tuned to match the properties of real geothermal fluids comprised of multiple chloride salts and noncondensable gases given the appropriate measured data. We are currently pursuing such a program for the Salton Sea reservoir in California.

ACKNOWLEDGEMENT

We thank the management of Unocal for permission to publish this paper.

APPENDIX

HENRY'S LAW CONSTANT

$$H_{sat} = P_{sat} \cdot \phi_{sat} \cdot \exp(\, HLSC / T)$$

$$HLSC = -491 + 3863 \cdot \rho_{H2O} - 150 \cdot \rho_{H2O} \cdot \exp[(273.15-T)/50]$$

where

H_{sat} = Henry's law constant for CO_2 along pure water saturation line

ρ_{H2O} = Density of liquid H_2O at saturation (g/cc)

T = Temperature (°K)

ACTIVITY OF WATER

$$a_{H2O} = 1 + A \cdot m_{NaCl} + B \cdot m^2_{NaCl}$$

$$A = 0.13635 - 1.3885e\text{-}3 \cdot T + 4.1784e\text{-}6 \cdot T^2 - 5.5362e\text{-}9 \cdot T^3 + 2.8178e\text{-}12 \cdot T^4$$

$$B = -0.01113 + 6.875e\text{-}5 \cdot T + 1.8375e\text{-}7 \cdot T^2 + 2.4087e\text{-}10 \cdot T^3 - 1.23545e\text{-}13 \cdot T^4$$

ACTIVITY COEFFICIENT OF CO_2

$$\ln(\gamma_{CO2*}) = B_{CO2} \cdot m_{CO2} + B_{NaCl} \cdot m^2_{NaCl}$$

$$B_{CO2} = -0.143 + 34.56/T$$

$$B_{NaCl} = 0.30912 - 2.04898e\text{-}3 \cdot T + 7.8867e\text{-}6 \cdot T^2$$

Here, m_{CO2} and m_{NaCl} are the molalities of carbon dioxide and sodium chloride in the solution. T is the temperature in °K.

H_2O-NaCl MOLAR VOLUME

$$\ln(V_{sat}) = V0 + V1\cdot\tau^{0.325} + V2\cdot\tau^{0.8915} + V3\cdot\tau^{0.825} + V4\cdot\tau + V5\cdot\tau^2 + V6\tau^3 + V7\cdot\tau^4 + V8\cdot\tau^5$$

$$\tau = 1.0 - T/T_c$$

$$V0 = 4.0208 + 3.30\cdot x_{NaCl}$$
$$V1 = -1.9286$$
$$V2 = -34.214$$
$$V3 = +20.1$$
$$V4 = +15.45 - 4.7\cdot x_{NaCl}$$
$$V5 = -1.2059$$
$$V6 = +0.63339$$
$$V7 = +0.0$$
$$V8 = +0.47437$$

The volume of compressed fluids is determined relative to the volume of the saturated fluid as follows:

$$V = V_{sat}\cdot(1.0 + C\cdot(P-P_{sat}))$$

$$C = -1.14e\text{-}6 / [\tau^{1.25} - 5.6\cdot x_{NaCl}{}^{1.5} + 0.005]$$

V and V_{sat} are in cc/gm-mole, T and T_c are in °K, P and P_{sat} are in psi, and x_{NaCl} is the mole fraction of sodium chloride in the solution.

PARTIAL MOLAR VOLUME OF CO_2

$$v_{CO2}^{\circ} = 37.36 - 7.109e\text{-}2\cdot T - 3.812e\text{-}5\cdot T^2 + 3.296e\text{-}6\cdot T^3 - 3.702e\text{-}9\cdot T^4$$

T = ° C, V = cc/g-mole

H_2O-NaCl MOLAR ENTHALPY

$$H_{NaCl} = V0 + V1\cdot\tau^{0.325} + V2\cdot\tau^{0.825} + V3\cdot\tau^{1.2165} + V4\cdot\tau + V5\cdot\tau^2$$

$\tau = 1.0 - T/T_c$

$$V1 = -1.9286$$
$$V2 = -34.214$$
$$V3 = +20.1$$
$$V5 = -1.2059$$

x_{NaCl} < 0.0089 ml pct

$$V0 = +17036 + 161850.\cdot x_{NaCl}$$
$$V4 = -138743. - 221842.\cdot x_{NaCl}$$

x_{NaCl} > 0.0089 ml pct

$$V0 = +17036. + 80511.\cdot x_{NaCl}$$
$$V4 = -140011. - 79426.\cdot x_{NaCl}$$

H_{NaCl} is in BTU/lb-mole, T and T_c are in °K, and x_{NaCl} is the mole fraction of sodium chloride in the solution.

CO_2(vapor) ENTHALPY

$$H_{CO2,v} = 298.833 + .2055\cdot T + (.03821\text{-}9.35e\text{-}5\cdot T + 6.875e\text{-}8\cdot T^2)\cdot(P-P_{sat})$$

Here, T is the temperature in °F and P is the pressure of carbon dioxide gas in psi. The resulting enthalpy is in BTU/lb.

STEAM ENTHALPY

The steam enthalpy is expressed as follows:

$$H_{steam} = H_{sat} + H_{superheat}$$

$$H_{sat} = 2083.81 + 1113.4\cdot\tau^{.325} + 7485.9\cdot\tau^{.825} + 7408.2\cdot\tau^{1.2165} - 14125.\cdot\tau - 4031.\cdot\tau^2 + 1832.7\cdot\tau^3 + 1184.8\cdot\tau^4 - 832.1\cdot\tau^5$$

$$\Delta H_{superheat} = (1.9976 + .04177\cdot P - 4.2979e\text{-}5\cdot P^2 + 7.9985e\text{-}7\cdot P^3)\cdot\Delta T - (5.3805e\text{-}7 + 7.1562e\text{-}5\cdot P + 2.575e\text{-}6\cdot P^2)\cdot\Delta T^2$$

$$\ln(T_r) = .13611\cdot\ln(P_r) + 7.4972e\text{-}3\cdot(\ln(P_r))^2 + 2.2713e\text{-}4\cdot(\ln(P_r))^3$$

$$\Delta T = T - T_{sat}$$
$$\tau = 1.0 - T_r$$
$$T_r = T_{sat}/647.067$$
$$P_r = P/220.52$$

Here, temperature is °K, the pressure is bar and enthalpy is cal/g.

CARBON DIOXIDE HEAT OF SOLUTION

The heat of solution for CO_2 is derived from the derivative(Denbigh, 1971) of our equilibrium expression for the K-value for carbon dioxide as follows:

$$H_{CO2,sol} = -R\cdot T^2\cdot\ln(K_{CO2}/P))dT$$

$$H_{CO2,sol} = -119.94 + 1.3324e\text{-}2\cdot T - 1.298e\text{-}2\cdot T^2 - 3.267e\text{-}5\cdot T^3 + 2.810e\text{-}8\cdot T^4$$

At temperatures greater than 650°F, the heat of solution changes rapidly and we add an additional term to the above relationship as follows:

$$H_{CO2,sol} = H_{CO2,sol\ @\ 650°F} + 44.86\cdot(T-650)$$

In these equations the temperature is °F and the heat of solution is BTU/lb. Our predicted values are close to those derived by Ellis and Golding(1963).

REFERENCES

1) Burnham, C. W., Holloway, R. J. and Davis, N. F., "Thermodynamic Properties of Water to 1000°C and 10,000 Bars", Geological Society of America, Special Paper Number 132, 1969

2) Chen, L. H., "Thermodynamic and Transport Properties of Gaseous Carbon Dioxide", Thermodynamic & Transport Properties of Gases, Liquids & Solids, Am. Soc. Mech. Eng., 1959, pp. 358-369

3) Denbigh, K., The Principles of Chemical Equilibrium, Cambridge University Press, 1971

4) Ellis, A. J. and Golding, R. M., "The Solubility of Carbon Dioxide above 100 C in Water and in Sodium Chloride Solutions", Amer. J. Sci., 1963, Vol. 261, pp. 47-60

5) Gehrig, M., "Phasenleichgewichte und PVT-Daten Ternarer Mishungen asu H_2O-CO_2-NaCl bis 3 Kbar und 550 C', Diss. Rer. Nat. Karlsruhe, 1980

6) Gillespie, P. C. and Wilson, G. M., "Vapor-Liquid and Liquid-Liquid Equilibria: Water-Methane, Water-Carbon Dioxide, Water-Hydrogen Sulfide, Water-n-Pentane, Water-Methane-n-Pentane", GPA RR-48, 1982

7) Haas, J. L., "Physical Properties of the Coexisting Phases and Thermochemical Properties of the H_2O Component in Boil in NaCl Solutions", Geological Survey Bull. 1421-A (1976)

8) Harvey, A. H. and Levelt-Sengers, J. M. H., "Correlation of Aqueous Henry's Constants from 0 degrees Centigrade to the Critical Point", AIChE Journal, 1990, Vol. 36, No.4, pp. 539-545

9) Marshall, W. M. and Jones, E. V., J. of Inorg. and Nucl. Chem., (1974) vol. 36, pp. 2313-2318

10) Mason, D. M. and Kao, R., "Correlation of Vapor-liquid Equilibria of Aqueous Condensates from Coal Processing" Thermodynamics of Aqueous Systems with Industrial Applications, ACS Symposium Series 133, 1980 pp. 107-138

11) Peng, D. Y. and Robinson, "Two- and Three-Phase Equilibrium Calculations for Coal Gasification and Related Processes", Thermodynamics of Aqueous Systems with Industrial Applications, ACS Symposium Series 133, 1980 pp. 393-413

12) Pitzer, K. S., Peiper, J. C. and Busey, R. H., "Thermodynamic Properties of Aqueous Sodium Chloride Solutions", J. Phys. Chem. Ref. Data, Vol. 13, No. 1 (1984), pp. 1-104

13) Pitzer, K. S. and Bischoff, J. L., "Liquid-Vapor Relations for the System NaCl-H_2O: Summary of the P-T-x Surface from 300 to 500 C", Amer. J. Sci. V 289 p. 217 (1989)

14) Potter, R. W., and Haas, J. L., J. Res. U.S. Geol. Survey, V 6, No 2 (1978)

15) Prausnitz, J. M., Lichtenthaler, R. N and Azevedo, E. G., "Molecular Thermodynamics of Fluid-Phase Equilibria", Prentice-Hall, N.J. (1986)

16) Takenouchi, S. and Kennedy, G. C., "The Binary System H2O-CO2 at High Temperatures and Pressures", Am. J. Sci., 1964, Vol. 262, pp. 1055-1074

17) Tanger, J. C. and Pitzer, K. S., Geochimica et Cosmochimica Acta, V 53 (1989)

18) Toedheide, K., Franck, E. U., "Das Zweiphasengebiet die Kritishe Kurve im System Kohlendioxid-Wasser bis au Drucken von 3500 bar", Z. Phys. Chem., 1963, Vol 37., pp. 387-401

19) Torquato, S. and Stell, G. R., "An Equation for the Latent Heat of Vaporization" Ind. Eng. Chem. Fundam., 1982, vol. 21, pp. 202-205

20) Vinsome, P. K., private communication.

21) Weibe, R. and Gaddy, V. L., "The Solubility in Water of Carbon Dioxide at 50, 75 and 100 degrees, at Pressures to 700 Atmospheres", Amer. Chem. Soc. J., 1939, Vol 61, pp. 315-318

22) Zawisza, A. and Malesinska, B., "Solubility of Carbon Dioxide in Liquid Water and of Water in Gaseous Carbon Dioxide in the Range 0.2-5 MPa and at Temperatures up to 473 K", J Chem. Eng. Data, 1981 Vol. 26, pp. 391-395

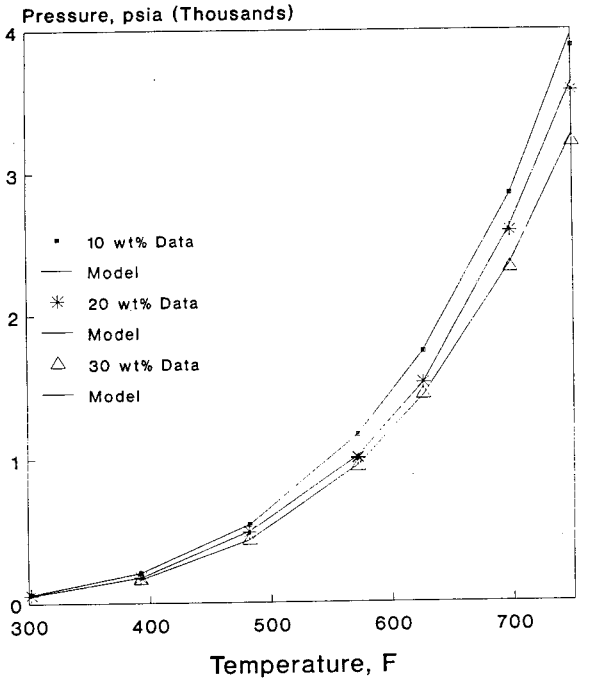

Fig. 1. Vapor pressure of NaCl solutions

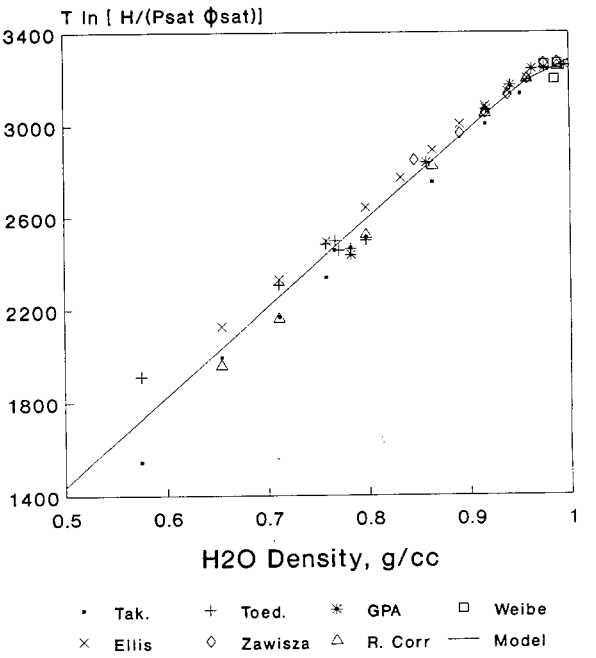

Fig. 3. Linear correlation for Henry's constant

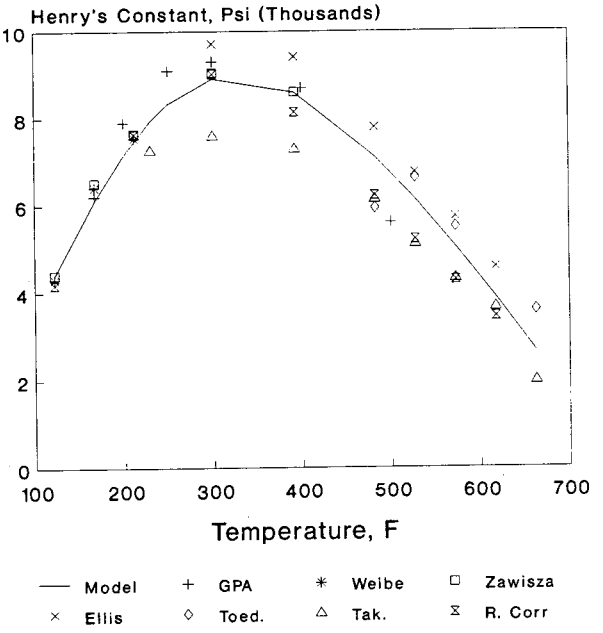

Fig. 2. Henry's constant vs. temperature (model and experimental data)

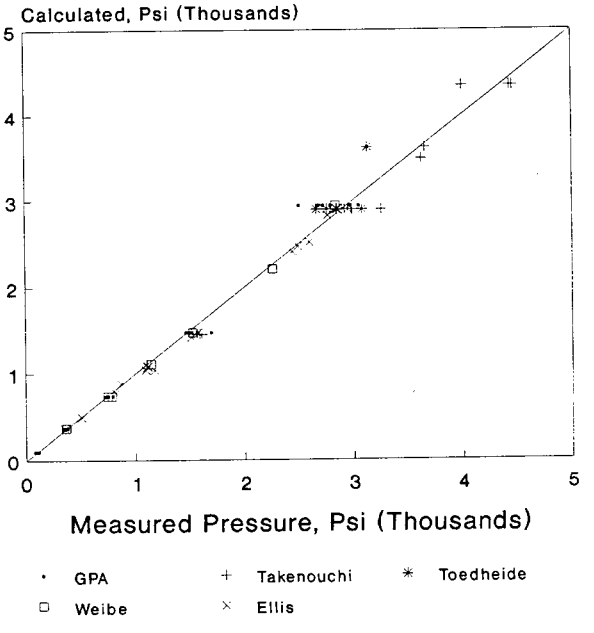

Fig. 4. Pressures for H_2O-CO_2 system (experimental vs. calculated)

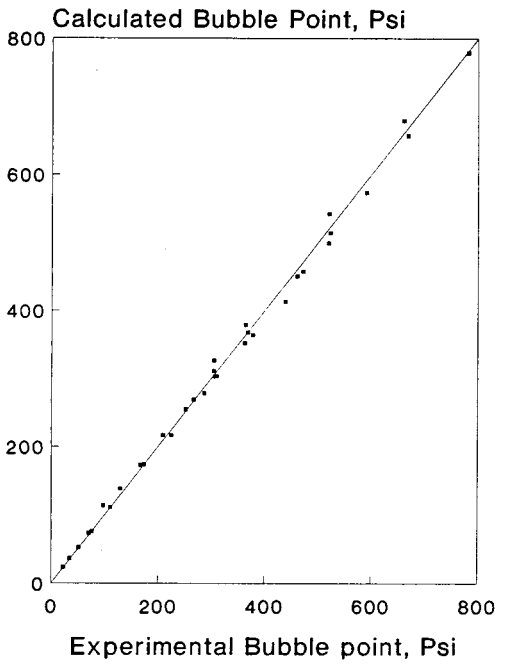

Fig. 5. Bubble point pressure for CO_2-H_2O system (calculated vs. Zawisza experimental data)

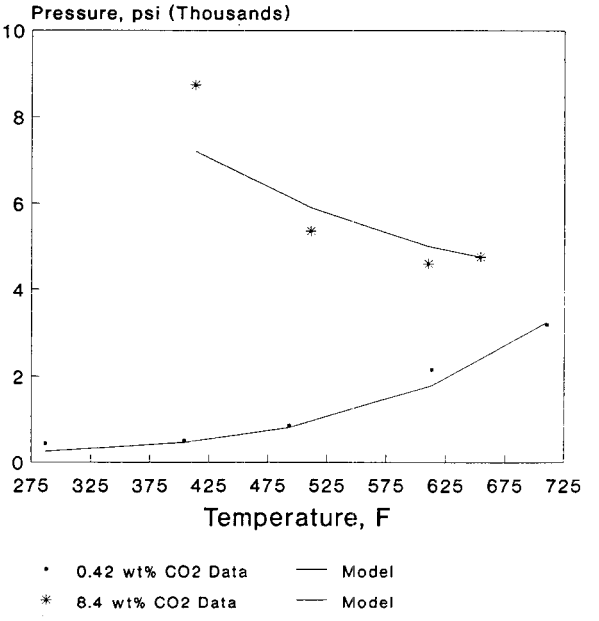

Fig. 7. Gehrig bubble point data (6.0 wt% NaCl-CO_2-H_2O system)

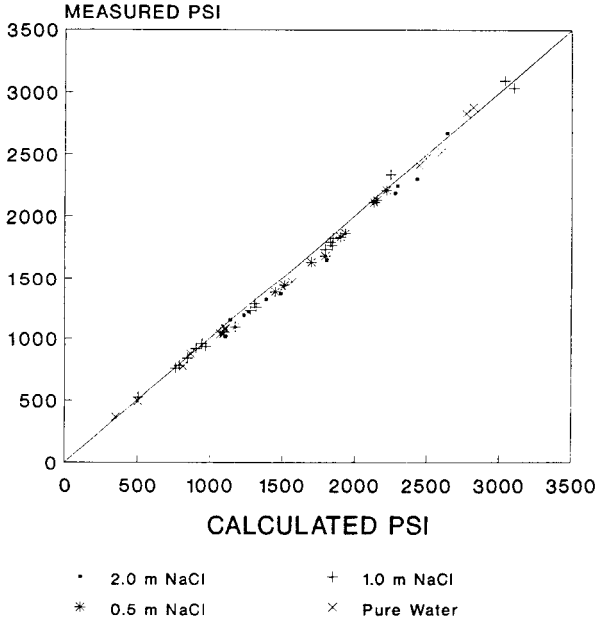

Fig. 6. Pressures for NaCl-H_2O-CO_2 system (Ellis data vs. calculated values)

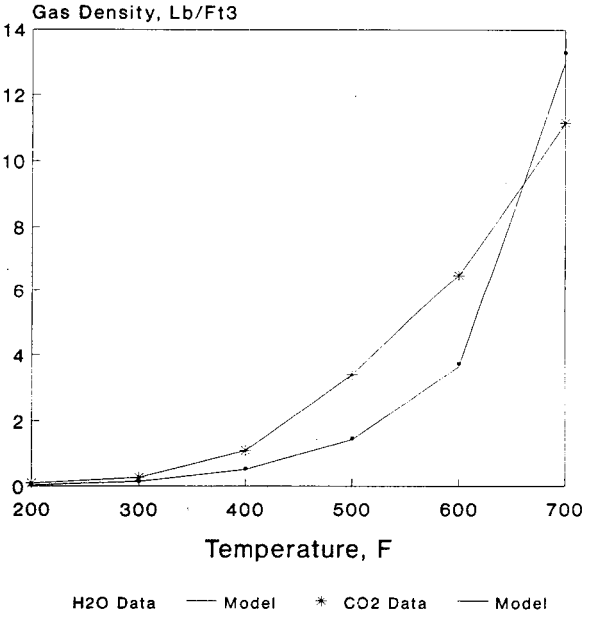

Fig. 8. Gas density from EOS (at home saturation pressure)

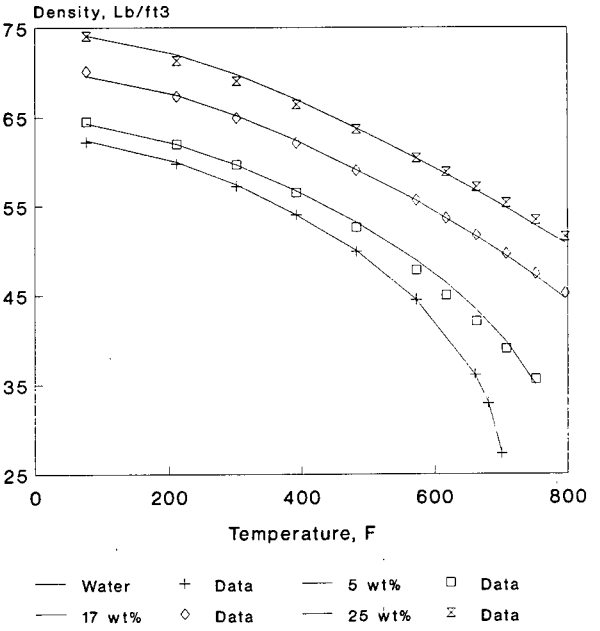

Fig. 9. Density of NaCl solutions (at water saturation pressure)

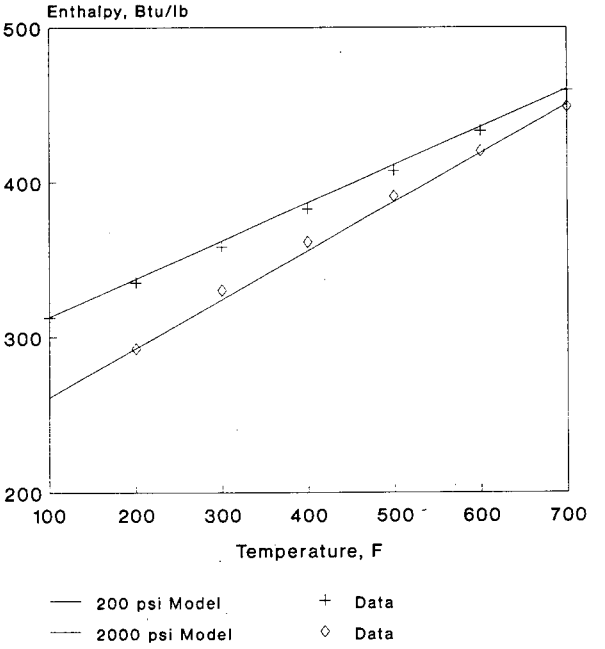

Fig. 11. Enthalpy of vapor-phase CO2

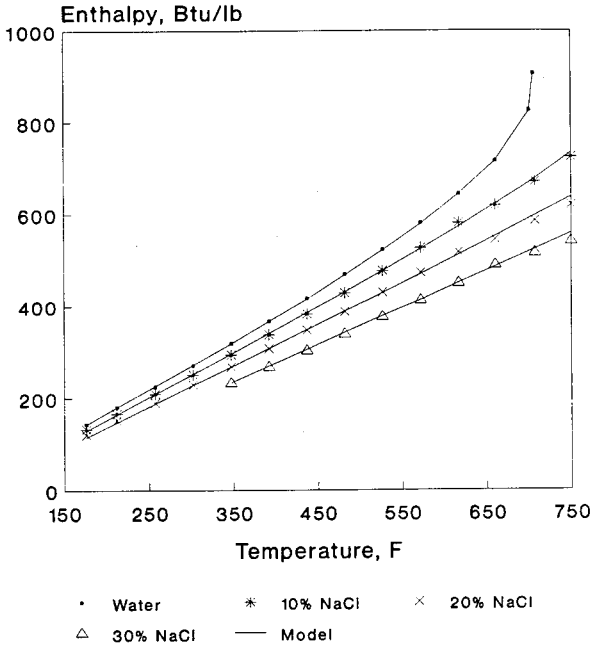

Fig. 10. Enthalpy of NaCl solutions

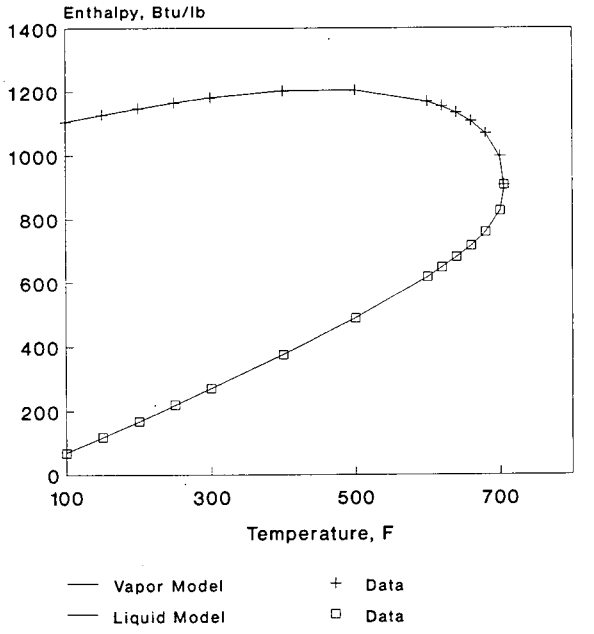

Fig. 12. Vapor and liquid enthalpy for water (at water saturation pressure)